Separable representation of the two-body Reid soft core T operator in terms of positive energy Weinberg states

George H. Rawitscher*
Department of Physics and Astronomy, University of Maryland, College Park, Maryland 20742
(Received 22 July 1988)

A separable approximation $T^{(S)}$ to the two-body T matrix of the form $\langle kT^{(S)}(E)k'\rangle = \langle kVk'\rangle + \sum_{s=1}^{S}\langle kV\Gamma_s(E)\rangle(1-\gamma_s)^{-1}\langle\Gamma_s(E)Vk'\rangle$ is examined, where V is the Reid soft core potential, Γ_s are the Weinberg eigenstates of the operator $G_0(E)V$ for positive energy E, and $\gamma_s(E)$ are the corresponding discrete complex eigenvalues. General projection techniques which improve the convergence of the sum above are considered. For the triplet state a nonlocal potential U is defined which in the $l=0$ channel represents the effect of the tensor coupling to the $l=2$ channel. It is found that the presence of U in the triplet state is responsible for the increased number of terms needed in the separable representation of T, as compared to the representation in the singlet state, where U is absent. The effect of U is largest for momenta less than 1 or 2 fm^{-1}.

I. INTRODUCTION

There is a long-standing puzzle concerning the number of terms needed for the separable approximation to the two-body scattering T operator. For uncoupled states, such as the singlet $^1S_0$, a rank of order 4 is sufficient to reach good accuracy, but for the coupled states, such as the $^3S_1$-$^3D_1$, a rank twice as large is required.[1] Why is this so?

The purpose of this paper is to compare the potentials in both states as far as the separable expansion properties are concerned. The analysis is made in terms of positive-energy Weinberg states.[2] The advantage of these states is that they provide a natural separable representation of the Green's functions G_V which are distorted by a potential V, which is valid both for a single or a coupled-channel situation. These Green's functions occur in the expression for the T operator

$$T(E)=V+VG_V(E)V \tag{1.1}$$

and also in the expression for the potential U which represents the effect of coupling of a channel space Q to a channel space P

$$U_{PP}(E)=V_{PQ}G_V^{(Q)}(E)V_{QP}\ . \tag{1.2}$$

Another useful property of the Weinberg state formalism is that the Weinberg eigenvalues γ_s which correspond to a potential V are dimensionless quantities which provide a measure of the strength of the potential at the energy E. The method is thus suitable to provide a comparison of the strengths of the potentials in the singlet and triplet nucleon-nucleon states. Another purpose is to examine the accuracy of the expansion of VG_VV. In the case that the potentials are of a Woods-Saxon or Gaussian-type the positive energy Weinberg state expansion converges quite rapidly,[3,4] but in the presence of repulsive cores the accuracy properties are as yet unknown.

There is a rich literature in the field of separable approximations to the nucleon-nucleon T operator or potentials.[1,5] One of the most popular representations is that of the Graz group.[6] It is based on the Ernst, Shakin, and Thaler (EST) method,[7] even though the latter is not without difficulties,[8] and uses analytic expressions for the form factors. An interesting generalization of the EST method to energy-dependent potentials has been given by Pearce.[9] A subtraction technique of the Noyes-Kowalsky–type has been introduced by the Bonn group[10] so that the separable part of the approximation to the T operator is of rank 1. Positive-energy Weinberg states have been used in the past for Hulthen,[2] Yukawa[2,11] square well,[3,12] Woods-Saxon,[13–15] and Gaussian potentials,[4] but probably because of the computational difficulty of treating complex eigenvalues and because the eigenvectors and form factors are energy dependent, their use is not widespread. Negative-energy Weinberg states have been used extensively,[16–21] as well as Gamow states.[22,23]

The methods based on Weinberg or Gamow stats give rise to form factors which are numerical rather than analytic, but they can be cast into analytical form through the use of Padé approximants.[24] Variational methods have also been employed,[25,26] in which case the form factors are analytical.

In Sec. II of this paper the formalism of the representation of T in terms of positive-energy Weinberg states in the full channel space is described and some pertinent properties of the T operator are given. Numerical applications to the nucleon-nucleon singlet and triplet states using the Reid soft core potential are presented in Sec. III. In particular, the effective potential which represents the effect of the tensor coupling between the $l=0$ and 2 channels is obtained. Section IV contains a summary and general discussion.

II. FORMALISM

The Weinberg states $|\Gamma_s\rangle$ are eigenfunctions of the operator G_0V and the corresponding eigenvalues γ_s

$$G_0(E)V|\Gamma_s(E)\rangle=\gamma_s(E)|\Gamma_s(E)\rangle\ . \tag{2.1}$$

Near the origin these functions are regular, and asymptotically they are determined by the properties of G_0, the

free Green's function. In the present application G_0 is asymptotically outgoing, and therefore the Weinberg states also have the same property. In the radial region where $V \neq 0$ the functions $|\Gamma_s\rangle$ have more and more nodes as s increases. This follows from the fact that V/γ_s are the potentials in the Schrödinger equation which the $|\Gamma_s\rangle$ obey. The larger the value of s, the smaller is the value of γ_s, the larger is the corresponding potential V/γ_s, and hence the more nodes the $|\Gamma_s\rangle$ have in the region where V is not zero. The quantities γ_s are dimensionless complex quantities such that V/γ_s has the appropriate "emissive" property which enables the $|\Gamma_s\rangle$ to be outgoing asymptotically. If V is purely attractive then γ_s is positive. If V has a repulsive component then some of the γ's have negative real parts.

In the coupled-channel case Eq. (2.1) reads

$$\sum_{n=1}^{N} G_{0n}(E_n)V_{nn'}|\Gamma_{n's}(E)\rangle = \gamma_s(E)|\Gamma_{ns}(E)\rangle \ , \tag{2.2}$$

where the E_n's are the channel energies and $G_{0n}(E_n)$ are the corresponding free Green's functions distorted only by the centripetal part of the potential for the angular momentum l_n which corresponds to channel n and $|\Gamma_{ns}(E)\rangle$ is the component of $|\Gamma_s\rangle$ in each channel n. The incident wave is assumed to be contained in channel 1 and T_{n1} represents the transition from channel 1 to channel n. The channel coupling generalization of the equation $T = V + VG_0T$ is

$$T_{n1}(E) = V_{n1} + \sum_{n'=1}^{N} V_{nn'}G_{0n'}(E_{n'})T_{n'1}(E) \tag{2.3}$$

whose solution is given by

$$T_{n1}(E) = V_{n1} \sum_{n',n''=1}^{N} V_{nn'}G_{n'n''}(E)V_{n''1}(E) \tag{2.4}$$

which is also written as

$$T_{n1} = V_{n1} + R_{n1} \ . \tag{2.5}$$

Here $V_{nn'}$ are the potentials which couple channel n to n' and $G_{n,n'}$ are the distorted channel Green's functions which contain the effect of all potentials. It can be shown[13] that these functions are given in terms of Weinberg states as

$$G_{nn'}(E) = \sum_s |\Gamma_{ns}(E)\rangle \frac{1}{1-\gamma_s} \langle \Gamma_{n's}(E)| \ . \tag{2.6}$$

As a consequence the term R defined in Eq. (2.5) is given by

$$R_{n1} = \sum_s |X_{ns}\rangle \frac{1}{1-\gamma_s} \langle X_{1s}| \ , \tag{2.7}$$

where the form-factors X are given by

$$|X_{ns}\rangle = \sum_{n'=1}^{N} V_{nn'}|\Gamma_{n's}\rangle \ . \tag{2.8}$$

The normalization of the Γ's is defined by

$$\sum_n \langle X_{ns}\Gamma_{ns'}\rangle = \gamma_s\delta_{ss'} \ , \tag{2.9}$$

where $\langle\ \rangle$ indicates integration from 0 to ∞ without complex conjugation of any of the functions in the integral. According to this definition, the magnitude of Γ is roughly proportional to $(\gamma_s)^{1/2}$. This is different from the use of some other authors, who define Sturmian functions χ_s which are equal to $X_s/(\gamma_s)^{1/2}$.

In order to define the polarization potentials U one also needs the Weinberg states $|\Gamma^{(Q)}_{ms}\rangle$ which are defined in the restricted channel space Q, i.e., $m \in Q$. These functions obey the analog of Eq. (2.2) where, however, n and n' are restricted to channel space Q. The corresponding channel Green's function $G^{(Q)}_{nn'}$ is given by the analog of Eq. (2.6) with Γ and γ replaced by $\Gamma^{(Q)}$ and $\gamma^{(Q)}$, respectively. The functions $X^{(Q)}$ are given by

$$|X^{(Q)}_{ns}\rangle = \sum_{m' \in Q}^{N} V_{nm'}|\Gamma^{(Q)}_{m's}\rangle \ , \tag{2.10}$$

where n is not restricted to belong to Q space. The polarization potentials $U_{nn'}(E)$ are then given by

$$U_{nn'}(E) = \sum_s |X^{(Q)}_{ns}\rangle \frac{1}{1-\gamma^{(Q)}} \langle X^{(Q)}_{1s}| \ . \tag{2.11}$$

In the triplet nucleon-nucleon case discussed below, the P space is chosen to represent the $l=0$ channel ($n=1$) and the Q space contains only the $l=2$ channel ($n=2$). If one defines the P-space potential

$$V^{(P)}_{11} = V_{11} + U_{11} \ , \tag{2.12}$$

then one can define the P-space Weinberg states $|\Gamma^{(P)}_s\rangle$ as being the eigenfunctions of $G_0V^{(P)}$

$$G_{01}(E_1)V^{(P)}_{11}|\Gamma^{(P)}_{1s}(E_1)\rangle = \gamma^{(P)}_{1s}(E_1)|\Gamma^{(P)}_{1s}(E_1)\rangle \ , \tag{2.13}$$

and one obtains for T the expression

$$T_{11} = V_{11} + U_{11} + R^{(P)}_{11} \tag{2.14}$$

with

$$R^{(P)}_{11} = \sum_s (V_{11} + U_{11})|\Gamma^{(P)}_{1s}\rangle \frac{1}{1-\gamma^{(P)}} \times \langle \Gamma^{(P)}_{1s}|(V_{11} + U_{11}) \ . \tag{2.15}$$

The quantities R_{11} and $R^{(P)}_{11}$ differ in that the Weinberg states and eigenvalues required for the expression (2.7) are defined in the whole channel space, while the corresponding quantities for $R^{(P)}$ are defined in the restricted P space, which in the presence case contains only the $l=0$ channel.

If the sum over s in Eq. (2.7) is cutoff at a finite number S then one obtains a rank S separable representation of R_{n1}, or equivalently of $(T\text{-}V)_{n1}$, and similarly for the expression (2.11) for U. The quantities $T\text{-}V$ and U are both nonlocal, and hence separable representations are likely to be useful. The potentials V can also be represented by[13,14]

$$V_{nn'}(r)\delta(r,r') = \sum_s X_{ns}(r)\frac{1}{\gamma_s}X_{n's}(r') \ , \tag{2.16}$$

which follows from the completeness of the Weinberg states in the region of the potentials.[2] Since V is local,

this expansion is not expected to converge as rapidly as the expansion for R, and the resulting alternate expression for T,

$$T_{n1}=\sum_s X_{ns}\frac{1}{\gamma_s(1-\gamma_s)}X_{1s}\ , \tag{2.17}$$

is not expected to converge as well either.

The momentum representation of the various quantities defined above is obtained in terms of the form factors

$$X_{ns}(k)\equiv\langle k_n|X_{ns}\rangle\equiv\int_0^\infty f_n(kr)X_{ns}(r)dr\ , \tag{2.18}$$

where the functions f_n are defined in terms of the spherical Bessel functions $j_l(z)$ as

$$f_n(z)=zj_{l_n}(z),\quad z=kr\ . \tag{2.19}$$

The momentum representation of T and V is defined accordingly as follows. If $Q_{n1}(r,r')$ is a general quantity, then the momentum representation of Q is

$$\langle kQ_{n1}k'\rangle\equiv\int_0^\infty f_n(kr)Q_{n1}(r,r')f_1(k'r')dr\,dr'\ . \tag{2.20}$$

Accordingly, the dimension of the momentum representation of V or T is energy$\times$length, which differs from definitions given more commonly which use, for f_n, an expression similar to Eq. (2.19) divided by k. The resulting dimension for V or T is energy$\times$(length)^3.

III. NUMERICAL RESULTS

The numerical evaluation of the eigenfunctions Γ and eigenvalues γ is performed by expanding the Γ's in terms of a set of basis states ϕ_{nj}, $j=1,2,\ldots,M$, defined in each channel n. These functions are denoted as "primitives," and they are defined as

$$\phi_{nj}(r)\propto f_n(K_{nj}r)\ , \tag{3.1}$$

where the f's are defined in Eq. (2.19) and the K's are complex wave numbers defined such that at a matching radius R the logarithmic derivatives of the ϕ_{nj}'s are equal to the logarithmic derivatives of outgoing Hankel functions which correspond to the energy and angular momentum of the scattered particle in channel n. In the same channel these functions are orthogonal in the radial range from 0 to R. They are normalized as described in previous work.[3,14,15] The real parts of K_{nj} are such that as j increases by one unit the corresponding ϕ_{nj} acquires one additional node in the interval 0 to R.

The expansion of the Γ's in terms of the ϕ's is

$$|\Gamma_{ns}\rangle^{(M)}=\sum_{j=1}^{M}c_{nj,s}^{(M)}|\phi_{nj}\rangle\ . \tag{3.2}$$

Expansion (3.2) is essentially a momentum representation in discrete complex momentum space.[14] The sum over j is truncated at the upper limit M, and hence it represents an approximation to the functions Γ, as well as to the other quantities such as the γ's, X's, and T's. The coefficients $c^{(M)}$ are the eigenvectors of the matrix $V^{(M)}$ whose elements are defined by

$$(V^{(M)})_{nj,n'j'}=\int_0^R\phi_{nj}(r)V_{nn'}(r)\phi_{n'j'}(r)\,dr\ , \tag{3.3}$$

and the corresponding eigenvalues $\gamma^{(M)}$ are M approximants to the Weinberg eigenvalues γ.

In the numerical applications described below, approximations to the integrals in Eq. (3.3) are obtained by setting the upper limit R to ∞,

$$(V)_{nj,n'j'}\approx\langle\phi_{nj}|V_{nn'}|\phi_{n'j'}\rangle\ . \tag{3.4}$$

This enables one to use analytic expressions for the resulting definite integrals and also to include the effect of the potential tail beyond R. In the case of the Reid soft core (RSC) potentials these expressions are obtained by extending the results given by Haftel and Tabakin[27] to the complex momentum space, as is described in Appendices A and B. A discussion of the numerical accuracy is given in Appendix C.

The nucleon-nucleon potentials have strong repulsive cores, which generate substantial Fourier components for large momenta. As a result the Weinberg eigenfunctions also have large momentum components, which in turn requires that the upper limit M in the summation over s in Eq. (3.2) be quite large, of the order of 50–80. This is shown in Table I which illustrates the convergence with M of the momentum representation of T for the triplet case. For a matching radius of $R=15$ fm a value of $M=75$ is needed to achieve stability in the third significant figure, while for $R=7.5$ approximately half as large a M value is required. This is not unreasonable, since a few expansion functions should have more than one node in the region of the repulsive core, which extends to about 0.5 fm. For $R=15$ fm the value of j for which the first zero of ϕ_{1j} occurs at 0.5 fm is equal to 30. Hence, a value of M twice as large is not unexpected. For $j=30$ the real part of the wave function K_{1j} equals 6.2 fm^{-1}. Hence, a value of K twice as large is still expected to play a role, and the momentum representation of V or of T for $k=15$ fm^{-1} is also expected to be non-negligible. This is indeed found to be the case, as is illustrated in Figs. 1–3. Most of this effect is due to the contribution from the repulsive core, whose effect is illustrated by the dash-dotted lines in Figs. 1–3. The repulsive core part of the potential is obtained by replacing the central, spin-orbit, and tensor parts of the RSC potential by one Yukawa term, respectively, so that for small values of the radial distance r each such terms equals the corresponding full potential to order r^{-1} and r^0. Further details are given in Appendix A.

The core part of the potential also has a large effect on the eigenvalues, as can be seen from Table II. In this table the negative values of γ are separated from the positive ones. The results for the core part of the potential for the triplet state are also shown. One sees that the latter are entirely negative, and their values are in close correspondence with the negative values of γ for the full triplet potential. For the singlet potential neither the negative nor the positive eigenvalues are as large in magnitude as the corresponding values for the triplet potential (in fact, they are smaller by about a factor of 2). But this result cannot directly be interpreted as evidence that the triplet potential is larger than the singlet one, since the matrices $V^{(M)}$ which define the eigenvalues are not of the same dimension. For $M=50$, for example, the size of

TABLE I. $\langle k'|T_{11}^{(M)}|k\rangle$[a] as a function of M.[b]

R[c]$=15$ fm, $E=5$ MeV

	$\langle 0.5\|T_{11}^{(M)}\|0.5\rangle$		$\langle 0.5\|T_{11}^{(M)}\|4.5\rangle$		$\langle 3.5\|T_{11}^{M}\|4.5\rangle$	
M	Re	Im	Re	Im	Re	Im
35	5.027	−25.18	−9.30	62.88	238.7	−163.9
45	5.315	−25.09	−10.44	65.00	233.3	−171.3
55	5.466	−25.04	−10.94	65.50	234.7	−172.6
65	5.501	−25.02	−11.04	65.52	235.0	−172.6
75	5.504	−25.02	−11.05	65.52	235.1	−172.6
	$\langle 0.5\|T_{21}^{(M)}\|0.5\rangle$		$\langle 0.5\|T_{21}^{(M)}\|4.5\rangle$		$\langle 3.5\|T_{21}^{(M)}\|4.5\rangle$	
M	Re	Im	Re	Im	Re	Im
45	1.256	−1.455	−10.01	3.834	9.997	172.9
55	1.261	−1.429	−10.13	3.804	8.782	174.3
65	1.261	−1.424	−10.13	3.796	8.553	174.5
75	1.262	−1.422	−10.14	3.791	8.488	174.4

$R=7.5$ fm, $E=5$ MeV

	$\langle 0.5\|T_{11}^{(M)}\|0.5\rangle$		$\langle 0.5\|T_{11}^{(M)}\|4.5\rangle$		$\langle 3.5\|T_{11}^{(M)}\|4.5\rangle$	
M	Re	Im	Re	Im	Re	Im
20	5.189	−25.10	−9.93	63.94	232.8	−167.1
35	5.508	−24.99	−11.02	65.28	234.4	−170.9
45	5.486	−24.94	−11.02	65.28	234.6	−171.0
55	5.512	−24.96	−11.09	65.24	234.3	−170.6
	$\langle 0.5\|T_{21}^{(M)}\|0.5\rangle$		$\langle 0.5\|T_{21}^{(M)}\|4.5\rangle$		$\langle 3.5\|T_{21}^{(M)}\|4.5\rangle$	
M	Re	Im	Re	Im	Re	Im
20	1.251	−1.453	−9.77	3.693	11.802	169.0
35	1.261	−1.399	−10.05	3.644	9.163	172.8
45	1.266	−1.410	−10.09	3.648	9.103	173.0
55	1.264	−1.401	−10.05	3.633	9.364	172.7

[a]The values of the momenta k' and k are in fm^{-1}; the value of $\langle k'|T|k\rangle$ is in MeV fm. The center-of-mass energy is 5 MeV. The momentum representation is defined in Eq. (2.20).
[b]M is the size of the space of the primitive functions ϕ.
[c]R is the radius where the boundary condition is imposed on the Sturmian primitive functions.

the matrix for the triplet case is 100×100 while for the singlet case it is 50×50.

In order to compare the strengths of the singlet and triplet potentials it is necessary to first project the triplet potential onto the $l=0$ channel. This is accomplished by introducing the polarization potential U_{11} which represents the effect of the coupling to the $l=2$ channel. The result is shown in Table III. The column for V_{11} lists the eigenvalues for the central part of the triplet potential in the absence of coupling to the $l=2$ channel. These eigenvalues are considerably larger than the ones for the singlet potential, indicating that the former is significantly larger than the latter. When U_{11} is added to V_{11} the eigenvalues become less negative, which shows that the effect of the tensor coupling to the $l=2$ channel has an attractive effect in the $l=0$ channel. This is to be expected since without the tensor coupling the deuteron would not be bound. The eigenvalues of $V_{11}+U_{11}$ are still somewhat larger than those for the singlet state. The difference is not very large, however: in both cases only three eigenvalues lie outside or near the unit circle. Also, the convergence of the corresponding R terms, i.e., R for the S state, Eq. (2.7), and $R^{(P)}$ for the triplet state, Eq. (2.15), is approximately the same, with three or four terms needed in order to achieve an accuracy of 1%. According to Eq. (2.14) the representation of T_{11} also requires the evaluation of U_{11}. The latter is represented by Eq. (2.11) for which the sum over s converges much more slowly than the sums for the terms R discussed above, as is shown below. Thus, the presence of the tensor coupling is identified as the main reason why the separable representation of the T matrix for the triplet state requires considerably more terms than that for the singlet state.

The relative importance of the terms V_{11}, U_{11}, and $R_{11}^{(P)}$ is described in Table IV. For low momenta such as 0.5 fm^{-1}, the three terms are comparable and they cancel each other so that their sum, T, is an order of magnitude smaller than V. For larger momenta U becomes small compared to V or R. The number of terms required in the sums over s for the various terms in order to achieve stability in the third significant figure is indicated in the table. That number is largest for U. As the relative importance of U decreases, the number of terms needed to calculate T also decreases. In Fig. 4 the rate of convergence of the sums over s required to obtain T is illustrat-

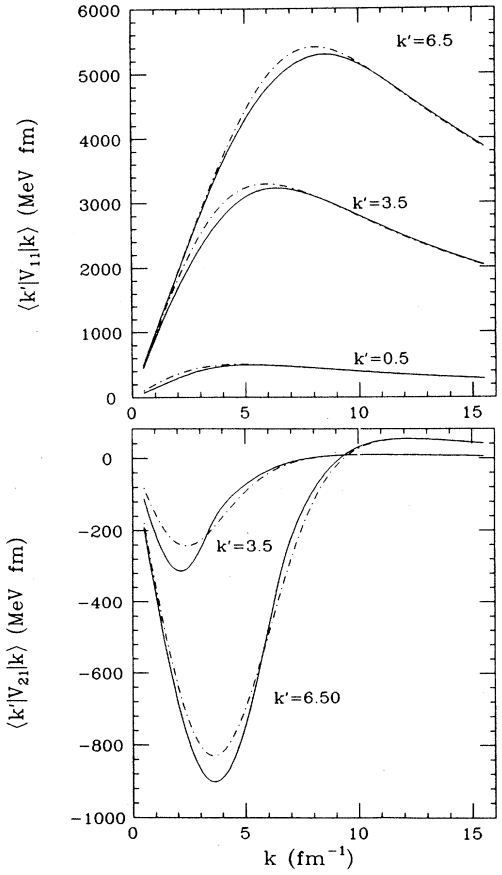

FIG. 1. Momentum representation of the Reid soft core potentials. V_{11} (V_{21}) is the $^3S_1$-$^3S_1$ ($^3D_1$-$^3S_1$) potential. The momentum representation is defined by Eq. (2.20). It is larger by a factor $k \times k'$ than more common definitions. The dashed-dotted line represents the results for the core part of the Reid potential, which is defined in Appendix A; the solid line represents the complete potential.

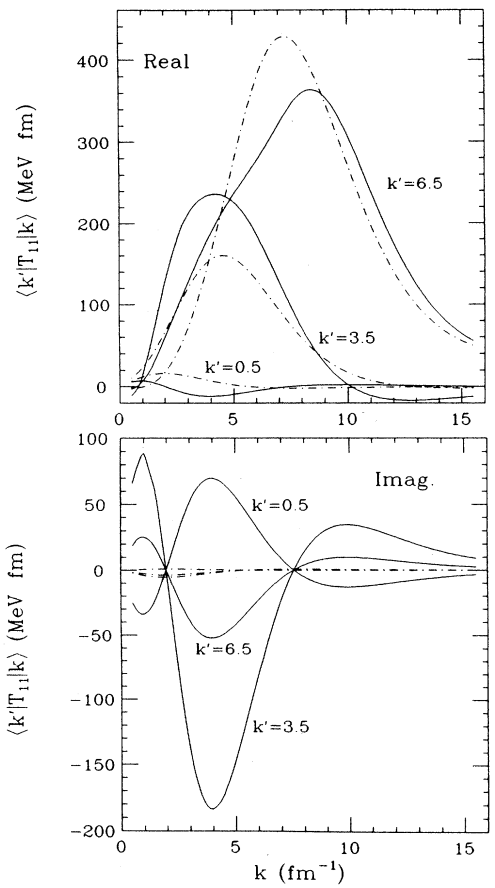

FIG. 2. Momentum representation of the T_{11} matrix for the complete (solid line) and core part (dot-dashed line) of the Reid soft core $^3S_1$-$^3D_1$ The notation is similar to Fig. 1.

ed. The number of stable significant figures achieved for T is shown on the horizontal axis, and the corresponding number of terms needed in the sum over s is shown in the vertical axis. The terms in the sums are arranged in order of decreasing absolute value of γ_s. The shaded rectangles connected by dashed lines indicate the result for the $^1S_0$ case. In this case the sum over s is given by Eq. (2.7) evaluated for the singlet state. For comparison, the convergence for the $^1S_0$ case obtained by Adhikari and Tomio[25] with an analytic form-factor method is illustrated by the unconnected shaded rectangles in the $\langle 0.5|T_{11}|0.5\rangle$ panel in Fig. 4. These points represent the accuracy for the phase shifts taken from line C of Table II of Ref. 25 for a center-of-mass energy of 12 MeV. Line C of that table represents the results for an approximation to T-V, and hence is of the same nature as the present calculation. The points marked O and connected by solid lines are based on Eq. (2.14) which makes use of the polarization potential U. This is denoted below as the O method. The results marked by the symbol P are obtained by a projection method described in Appendix D, which, like the O method, reduces the size of the matrices which have to be diagonalized, compared to the size of the matrices in the full channel space. One sees from Fig. 4 that the accuracy properties of the P and O methods are approximately the same, and that the size (or rank) of the expansion needed to achieve a given accuracy for T_{11} decreases for the higher momenta, where it approaches the accuracy for the singlet state. This result is consistent with the observation made above that the polarization potential U becomes relatively unimportant for the higher momenta. For the off-diagonal part of the T matrix the accuracy, illustrated in Fig. 5, is not as good.

The overall accuracy properties of the expansion of T_{11} and T_{12} are summarized in Table V, which gives the number of terms needed to achieve an accuracy of 1%. However, it should be kept in mind that the rank of the separable representation of the two-body T matrix required so as to achieve the % accuracies described above is not directly related to the rank of the representation of the two-body T matrix which is needed to provide a given accuracy in the calculation of three-body observables. This question requires a separate study which goes beyond the scope of the present investigation.

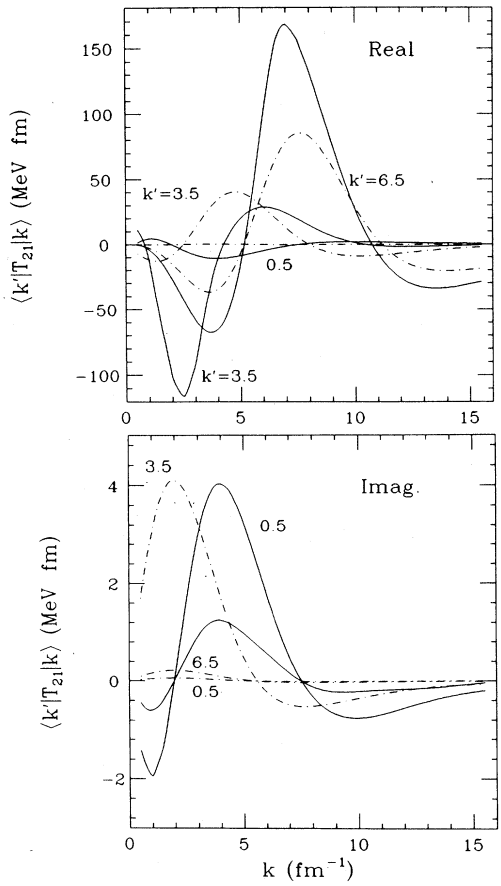

FIG. 3. The same as Fig. 2 for T_{21}. The result for $k'=3.5$ fm^{-1}, full RSC potential is not shown because its value is too large. Its maximum value is 185 MeV fm near $k=3.0$ fm^{-1} and its minimum is -35 MeV fm at $k=10$ fm^{-1}.

IV. SUMMARY AND CONCLUSIONS

It is shown that the rank of the representation of the T matrix in the triplet state is larger than that in the singlet state because of the effect of the tensor coupling between the $l=0$ and 2 channels. It is thus likely that improvements in the methods which start from a separable representation of the potential V in terms of a set of functions such as positive- or negative-energy Weinberg states, Gamow states, etc., and then obtain the corresponding separable representation of T, are not going to yield ranks which are much lower than the ones achieved at present.[19–26]

The line of reasoning developed here consists in obtaining the polarization potential U which represents the effect of the tensor coupling in the $l=0$ channel, (method O) and then show that the presence of U is responsible for the increased rank of the representation. Table IV is most relevant for this argument. The projection method P, in which U is not explicitly calculated, gives a similar rank for the representation, and hence it is assumed that other methods also contain the detrimental effect of U implicitly.

In order to obtain a viable low-rank method of solving three-body problems which use as input the two-body T matrices, it is therefore desirable to seek other types of separable representations for T. One very promising candidate is the W-matrix method of Haberzettl, Sandhas, and co-workers.[10] In this method the half on-shell portion of T is given by a rank one separable expression, and the remainder, called R, makes only a small contribution to the three-body results in the cases which have been examined thus far.[10] These cases do not include explicitly the effect of the tensor coupling, and a study of R under these conditions is in progress.[28] A second promising approach is to use the quasi-particle method of Weinberg.[2,3] The idea is not to seek a fully separable representation of T, but only for a part of T which corresponds to the large Weinberg eigenvalues. The rest is to be included perturbatively in the calculation of three-body observables.[17,29]

A further result which emerges from the present study is that calculations of the polarization potential U in terms of positive energy Weinberg states are viable and accurate. The calculation of U in terms of negative-energy Weinberg states are also feasible.[30] The knowledge of U is of interest, for example, in the analysis of why different nucleon-nucleon potentials give a different triton binding[31] since the various potentials differ mainly in the amount of tensor coupling.

ACKNOWLEDGMENTS

The author gratefully acknowledges useful discussions and correspondence with G. Pisent which motivated this investigation and with Z. Kuruoglu, E. F. Redish, J. Tjon, and S. Wallace while the work was in progress at the University of Maryland. Conversations with L. Canton were especially useful to clarify the relation between the use of positive- and negative-energy Weinberg states. The hospitality of the University of Maryland Nuclear Theory Group, and the partial support of the U.S. Department of Energy, the University of Maryland Computer Science Center, and the Computer Center of the University of Connecticut is also very much appreciated.

APPENDIX A: THE CORE PART OF THE REID SOFT CORE POTENTIAL

The Reid potential[32] is composed of a central, spin-orbit, and tensor part, which in turn are given as a combination of three types of functions:

$$Y_1(m,x)=\exp(-mx)/x \ , \tag{A1}$$

$$Y_2(m,x)=(m/x+1/x^2)Y_1(m,x) \ , \tag{A2}$$

$$Y_3(m,x)=(m^2+3m/x+3/x^2)Y_1(m,x) \ , \tag{A3}$$

where x is related to the radial distance r by

$$x=\kappa\times r \tag{A4}$$

and where[32] $x=0.7$ fm^{-1}. The central and spin-orbit parts of the Reid soft core potential for the triplet case are given by

$$V_C(r)=\sum_{m=1}^{6} A(m)Y_1(m,x) \ , \tag{A5}$$

TABLE II. Weinberg eigenvalues, γ_S, $E=5$ MeV, $R=15$ fm, $M=75$.

	$^3S_1$-$^1D_1$ Full potential			$^1S_0$ Full potential			$^3S_1$-$^3D_1$ Core potential	
	Re	Im		Re	Im		Re	Im
s			s			s		
1	−27.02	−2.32	1	−14.91	−0.96	1	−28.73	−2.94
2	−5.65	−0.18	2	−1.86	−0.04	2	−6.06	−0.30
3	−2.66	−0.09	4	−0.19	0.00	3	−3.19	−0.16
5	−1.15	−0.05				4	−1.81	−0.00
6	−0.84	−0.06				5	−0.97	−0.06
8	−0.42	−0.07				6	−0.55	−0.00
9	−0.24	−0.02				7	−0.32	−0.02
10	−0.20	−0.00				8	−0.16	−0.00
11	−0.12	−0.01				9	−0.12	−0.00
13	−0.07	−0.01				10	−0.04	−0.00
4	1.13	0.35	3	0.77	0.38			
7	0.26	0.05	4	0.11	0.03			
12	0.12	0.02	6	0.04	0.01			
14	0.07	0.01	7	0.02	0.01			
16	0.04	0.01	8	0.01	0.00			
18	0.03	0.00	9	0.01	0.00			

$$V_{\mathrm{SO}}(r)=\sum_{m=4}^{6} B(m)Y_1(m,x)\ , \tag{A6}$$

and the tensor part is of the form

$$V_T(r)=\sum_{m=4}^{6} C(m)Y_1(m,x)+G[Y_3(1,x)-3Y_2(4,x)]\ , \tag{A7}$$

where $A(m)$, $B(m)$, $C(m)$, and G are constants given by Reid and m assumes integer values from 1 to 6.

In the limit in which $mx \ll 1$ the exponential in $Y_1(m,x)$ can be expanded in a power series in x, and the terms in the various potentials can be regrouped in powers of x^{-1}, x^0, and x. These terms can be reexpressed in the form $A(\lambda)Y_1(\lambda,x)$ and by, in turn, expanding the exponential in $Y_1(\lambda,x)$ and identifying coefficients of x^{-1} and x^0, one obtains the value of $A(\lambda)$ and λ. No problems arise in the tensor term since in the term in square brackets the powers of x^{-3} and x^{-2} cancel exactly. One obtains

$$V_i^{(C)}=A_i(\lambda_i)Y_1(\lambda_i,x),\quad i=C,\ \mathrm{SO},\ T\ ,$$

where the values of A_i and λ_i are given in Table VI.

APPENDIX B: ANALYTIC INTEGRALS FOR COMPLEX WAVE NUMBERS

The evaluation of integrals of the type

$$\int_0^\infty f_{L_2}(K_2'r)r^{-1}\exp(-\lambda' r)f_{L_1}(K_1'r)dr = I^{(1)}_{L_2L_1}(K_2,\lambda,K_1) \tag{B1}$$

will be described in this appendix. The functions f are defined in Eq. (2.19) and the wave numbers K_1' and K_2' can be complex provided that the integral exists, i.e., if

$$|\mathrm{Im}(K_2')|+|\mathrm{Im}(K_1')|<\lambda'\ . \tag{B2}$$

By expressing the wave numbers K_2', K_1', and the decay length λ' in units of κ [see Eq. (A4)], $K_i=K_i'/\kappa$ $(i=1,2)$ and $\lambda=\lambda'/\kappa$, the integral above becomes the $i=1$ version of the general type of integrals discussed in this appendix:

$$I^{(i)}_{L_2L_1}(K_2,\lambda,K_1)=\int_0^\infty f_{L_2}(K_2x)Y_i(\lambda,x)f_{L_1}(K_1x)dx\ , \quad i=1,2,3\ . \tag{B3}$$

The function Y_i have been defined in Eqs. (A1)–(A3).

The notation is similar to that of Haftel and Tabakin,[27]

TABLE III. Weinberg eigenvalues γ_s in the space $l=0$ for $E=5$ MeV.

	$^1S_0$		$^3S_1$-$^3D_1$ V_{11}		$^3S_1$-$^3D_1$ $V_{11}+U_{11}$	
s	Re	Im	Re	Im	Re	Im
1	−14.91	−0.96	−26.00	−2.25	−20.90	−1.44
2	−1.86	−0.04	−4.19	−0.22	−1.81	−0.02
3	0.77	0.38	−0.76	−0.01	1.15	0.63
4	−0.19	0.00	0.32	0.15	0.14	0.01
5	0.11	0.03	−0.12	−0.00	0.10	0.03
6	0.04	0.01	0.04	0.01	−0.10	0.00

TABLE IV. Relative importance of terms U and R.[a]

$E_{c.m.}$	5 MeV				50 MeV		
			$\langle 0.5\|X_{11}\|0.5\rangle$[b]				
X	Real	S	Im	X	Real	S	Im
V	70.14		0	V	70.14		
U	−42.48	11	−0.08	U	−48.71	12	−8.16
R	−21.83	4	−24.96	R	−33.07	5	−4.50
T	5.47	12	−25.04	T	−11.64	12	−12.66
			$\langle 0.5\|X_{11}\|4.5\rangle$[b]				
X	Real	S	Im	X	Real	S	Im
V	489.3		0	V	489.3		
U	−78.43	9	0.01	U	−77.17	8	0.72
R	−421.8	6	65.49	R	−396.89	6	28.76
T	−10.94	12	65.50	T	15.30	10	29.48
			$\langle 3.5\|X_{11}\|4.5\rangle$[b]				
X	Real	S	Im	X	Real	S	Im
V	2953	0	0	V	2953		
U	−471.87	6	0.045	U	−473.9	8	−0.10
R	−2247	6	−172.6	R	−2333	3	−110.8
T	234.70	9	−172.59	T	145.8	8	−110.9

[a]The terms U and R are defined in Eqs. (2.11) and (2.15). The value of T is given by the sum of the two results. The momentum representation is defined in Eq. (2.20). The number of terms in the real part of the sums (2.11), (2.15), and (2.14) needed to achieve stability in the third significant figure for the momentum representation of U, R, and T, respectively, is denoted by S. The matching radius R is 15 fm. The number of primitives is $M=55$.

[b]X denotes either one of the quantities V, U, R, or T; the numbers indicate the values of the momenta k and k' in units of fm, the result $\langle k|X|k'\rangle$ is in units of MeV fm. Only the channel-1 to channel-1 transitions are included in this table.

with the exception that the integrals I defined in that reference have to be multiplied by the factor $K_1 \times K_2$ in order to become equal to the I's defined here.

The recursion relations between the I's for various L values, given in Ref. 27, are still valid for the case that the wave numers K are complex, but the values for special cases of L, needed to obtain the results for general L, have to be revised. The results needed are as follows:

$$I_{LL}^{(1)}(K_2,\lambda,K_1)=\tfrac{1}{2}Q_L(z)\ , \tag{B4}$$

where

$$z=(K_1^2+K_2^2+\lambda^2)/(2K_1K_2)\ , \tag{B5}$$

$$I_{20}^{(1)}(K_2,\lambda,K_1)=\{6K_1/K_2+K_2^{-2}[3\lambda^2-3K_1^2+K_2^2]Q_0(z) +3i\lambda K_1K_2^{-2}\ln z_2\}/4\ , \tag{B6}$$

where

$$z_2=[(\lambda+iK_2)^2+K_1^2]/[(\lambda-iK_2)^2+K_1^2] \tag{B7}$$

and the Q's are the Legendre functions of the second kind. Equation (B6) replaces Eq. (A8) in Ref. 27, otherwise all other equations remain the same.

The procedure to arrive at the results above consists in decomposing the integrals I for low values of L in terms of exponential integrals of the type

$$\int_0^\infty x^{-n}\exp(\Lambda x)dx=\varepsilon^{-n+1}E_n(\varepsilon\Lambda)\ ,$$

where $E_n(z)$ is defined in Ref. 33 and Λ is $\lambda\pm iK_1\pm K_2$. By making use of the recursion relations between E_n for various values of n, and by taking the appropriate limit for $\varepsilon\to 0$, explicit expressions for $I_{00}^{(1)}$, $I_{22}^{(1)}$, and $I_{20}^{(1)}$ were obtained. The first two of these results served to verify the validity of Eq. (B4). In the limit that the wave numbers are real, Eq. (B6) agrees with Eq. (A8) of Ref. 27. A further check consisted in calculating the integrals

$$\int_0^\infty f_{L_1}(K_1'r)V_x(r)f_{L_2}(K_2'r)dr$$

for the Reid potentials defined in Eqs. (A5)–(A7) with $X=C$, SO, or T for the $^3S_1$-$^3D_1$ case numerically on a radial mesh from $r=0$ to $R=15$ fm with complex wave numbers K_1' and K_2', and comparing the result with the analytical expressions developed in this appendix. Excellent agreement between the two methods was obtained.

APPENDIX C: NUMERICAL INFORMATION

The calculation is performed on an IBM 3084K at the University of Connecticut Computing Center in double precision. The eigenvalues and eigenvectors are obtained by the EIGCC subroutine from the International Mathematical and Statistical Libraries (IMSL) Library, in double precision, and the solution of algebraic equations is performed by LEQ2C also from IMSL. A run which calculates the representations of T both via the projection method P and by means of Eqs. (2.5) plus (2.7),

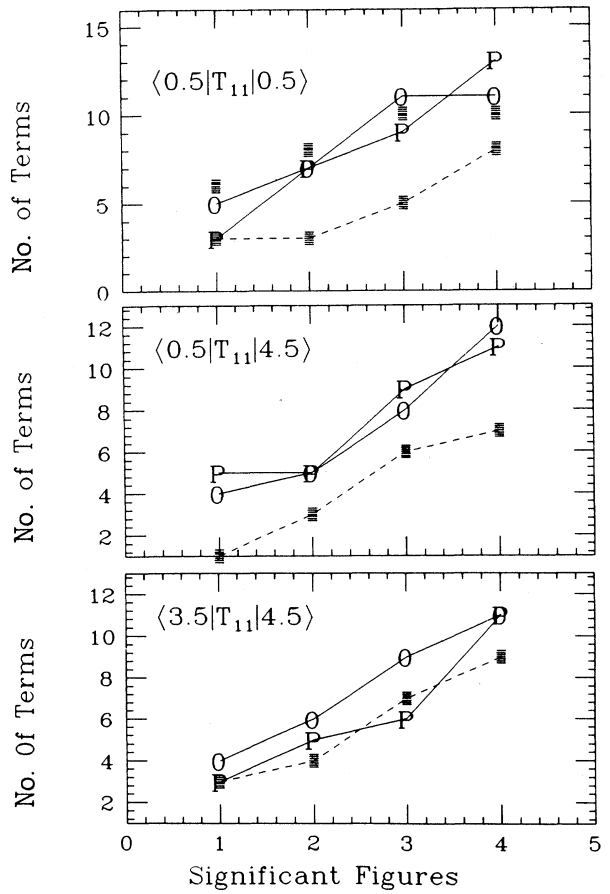

FIG. 4. Accuracy of $\langle k|T_{11}|k'\rangle$ at $E_{cm}=5$ MeV for various combinations of k and k' in fm^{-1}. The horizontal axis indicates the number of significant figures for which stability in T is achieved, after rounding, and the vertical axis indicates the corresponding number of terms needed in the sum for T-V. The shaded rectangles connected by the dashed lines indicate the results for the uncoupled $^1S_0$ case. The other shaded rectangles indicate the results obtained in Ref. 25 by a variational analytic method for the $^1S_0$ elastic phase shifts. The points marked P and O are obtained by the projection methods P and O described in Appendix D. Method O involves the nonlocal potential U. The boundary condition radius R equals 15 fm, the results for O are obtained with a size of the primitive basis of $M=65$, and for all other results $M=75$.

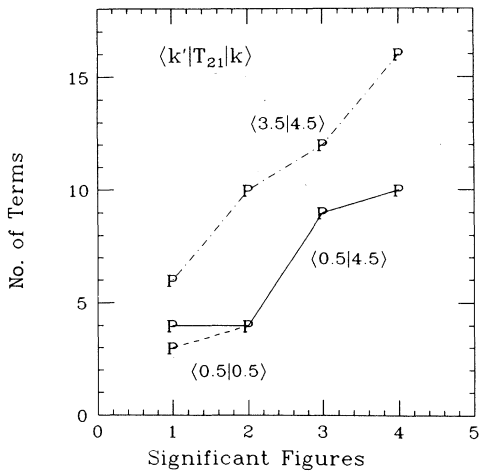

FIG. 5. Same as Fig. 4 for the 1→2 transition. The (k,k') combinations are indicated in the figure next to each line in units of fm^{-1}. Only projection method P is illustrated.

using a basis of 75 primitives, takes approximately 70 s of CPU time. If M is reduced from 75 to 35, the CPU time reduces to 32 s.

Checks on the code are as follows.

(a) The accuracy of the subroutines which produce the wave numbers K_{nj} for the primitive functions has been tested in a previous accuracy test[4] of the positive-energy Weinberg expansion method for solving coupled equations, and internal accuracy to better than 10 significant figures was achieved.

(b) The consistency between the results obtained for the T matrix using Eq. (2.5) plus (2.7) and (2.17) is a confirmation that no programming errors are present. The agreement between the two methods shows that Eq. (2.17) is numerically satisfied in the range of momenta examined. Similarly, the good agreement for T between the projection method P and the effective potential method O is another internal consistency test which checks the code for Eqs. (2.10)–(2.15). The fact that Eq. (2.17) is not numerically as stable as Eq. (2.5) plus (2.7), is an indication of the presence of numerical errors connected to the higher eigenvalue indices s, for which the eigenvalues γ_s are small. In the projection method the results are more stable than for the full channel space, and the quantities

TABLE V. Accuracy summary. Number of terms in sum[a] needed to achieve a relative error in $\langle k|T|k'\rangle$ equal to or less than 1%.

cm energy	5 MeV				50 MeV			
	$^3S_1$-$^3D_1$		$^1S_0$		$^3S_1$-$^3D_1$		$^1S_0$	
	Re	Im	Re	Im	Re	Im	Re	Im
$\langle 0.5\|T_{11}\|0.5\rangle$	7	5	3	3	8	8	5	5
$\langle 0.5\|T_{11}\|4.5\rangle$	6	5	4	3	9	8	5	3
$\langle 3.5\|T_{11}\|4.5\rangle$	5	5	4	3	7	7	3	4
$\langle 0.5\|T_{21}\|0.5\rangle$	7	6			7	10		
$\langle 0.5\|T_{21}\|4.5\rangle$	4	6			9	14		
$\langle 3.5\|T_{21}\|4.5\rangle$	8	4			6	6		

[a]For the singlet case Eq. (2.5) plus (2.7) are used. For the triplet case the projection method P is used, as defined in Appendix D. The boundary condition radius is $R=15$ fm, the number of primitive functions is $M=75$.

from the full channel space are weighted by a factor γ_s, i.e., the high s values are deemphasized.

(c) Comparison with the T-matrix results of a code developed at the University of Maryland,[34] to be denoted as EFR. The comparison was made at a center-of-mass energy of 50 MeV, for which the value of the on-shell momentum is 1.098 fm^{-1}. EFR's code solves the Lippmann-Schwinger Eq. (2.3) for T in momentum space, for a mesh of momentum values k ranging from 0.030 to 23.983 fm^{-1}. Our results (GR) use a boundary condition radius $R=15$ fm, the number M of primitives is 75, EFR's momenta k and k' for which the $\langle k|T|k'\rangle$ values are to be compared with GR's were read into GR's program. The comparison was made for T_{11} for the full triplet potential, for a range of momenta ranging from 0.152 to 11 fm^{-1}. The agreement between the two codes was better than 1% for most combinations of k and k', with a few exceptions where the agreement was better than only 2%. These few points did not, however, show a systematic trend. Values for T_{21} or T_{22} were not available for comparison.

APPENDIX D: THE PROJECTION METHOD P

Given an operator O_{n1} which acts to the right on functions in space 1, and to the left on functions in space n, one can construct a separable representation of O by introducing a set of functions $\chi_t^{(i)}$ and potentials $V^{(i)}$ in each of the two spaces i ($i=1$ or n), with $t=1,2,\ldots,$ such that the functions χ are V orthogonal

$$\langle \chi_t^{(i)} V^{(i)} \chi_{t'}^{(i)} \rangle = \delta_{tt'} , \tag{D1}$$

TABLE VI. The values of A_i and λ_i.

Type	A_i (MeV)	λ_i (dimensionless)
C	6831.505	6.879 168
SO	−2004.19	6.707 428
T	−1567.6105	5.934 862

and such that they form a complete set in the regions of space where the operator O is nonzero. The desired expansion is

$$O_{n1} = \sum_{t,t'} V^{(n)} \chi_t^{(n)} > P_{tt'}^{(n,1)} < \chi_{t'}^{(1)} V^{(1)} . \tag{D2}$$

In view of Eq. (D1), the elements of the matrix P are given by

$$P_{tt'}^{(\alpha)} = \langle \chi_t^{(n)} O_\alpha \chi_{t'}^{(1)} \rangle , \tag{D3}$$

where the symbol α Is used to denote the combination $(n,1)$. the expansion (D2) has the nature of a projection of O onto the space of the functions χ. In the application of this projection method to the $^3S_1$-$^3D_1$ case the operator O_α is set equal to R_α defined in Eq. (2.7), and the potential $V^{(i)}$ are the diagonal potentials V_{ii} in channels $i=1$ and 2. The corresponding functions $\chi^{(i)}$ are proportional to the single-channel Weinberg functions $\Gamma_t^{(i)}$ which correspond to $V^{(i)}$:

$$\chi_t^{(i)} = \Gamma_t^{(i)} / \sqrt{\gamma_t}, \quad i=1,2 . \tag{D4}$$

TABLE VII. Q and P Weinberg eigenvalues[a] and projection eigenvalues[a] p^P and p^O for the full $^3S_1$-$^3D_1$ case at $E_{cm}=5$ MeV.[b]

	$\gamma_s^{(Q)}$		$\gamma_s^{(P)}$		p_s^O		p_s^P	
s	Re	Im	Re	Im	Re	Im	Re	Im
$E_{cm}=5$ MeV								
1	−3.39	4.6 (−4)	−20.90	−1.44	12.52	−0.17	−2.29	4.02
2	−0.82	2.7 (−4)	−1.81	−0.02	−0.75	1.56	2.13	0.09
3	−0.16	−1.0 (−5)	1.15	0.63	−1.27	−0.08	−0.96	−3.1 (−3)
4	−0.08	−1.7 (−3)	0.10	0.03	−0.83	−0.01 (−4)	0.72	0.02
5	−0.03	−5.8 (−4)	−0.10	0.00	0.71	0.03	−0.86	−4.8 (−3)
6	−0.02	−1.0 (−3)	0.03	0.01	0.39	0.06	−0.77	−1.3 (−3)
7	−0.01	−6.1 (−4)	0.14	0.01	0.27	0.02	−0.45	−1.1 (−3)
8	−0.01	−3.7 (−4)	0.01	0.00	−0.17	−3.6 (−4)	0.42	0.03
9	−0.00	−2.4 (−4)	0.00	0.00	0.18	−6.0 (−3)	0.25	0.01
$E_{cm}=50$ MeV								
1	−3.49	−1.8 (−3)	−20.59	−5.06	9.50	−0.34	1.56	2.68
2	−0.87	−5.5 (−3)	−1.97	−0.15	−1.23	−0.07	−0.05	1.93
3	−0.17	−6.8 (−3)	0.13	0.95	−0.82	−0.02	−0.96	−0.01
4	−0.06	−9.4 (−2)	−0.10	0.00	0.05	0.67	0.75	0.28
5	−0.02	−1.8 (−2)	0.06	0.06	0.80	0.18	−0.87	−0.01
6	−0.02	−2.7 (−3)	0.02	0.01	0.42	0.10	−0.78	−6.7 (−3)
7	−0.01	−6.3 (−3)	0.01	0.00	0.26	0.06	−0.46	−4.9 (−2)

[a]The meaning of the operators and eigenvalues is described in Appendix D.

[b]The matching radius R has a value of 15 fm for all cases. The results in the first three columns are calculated with $M=55$. For the last column (p^P), $M=75$. The negative quantities in the parentheses indicate the power of 10 by which the entry is to be multiplied.

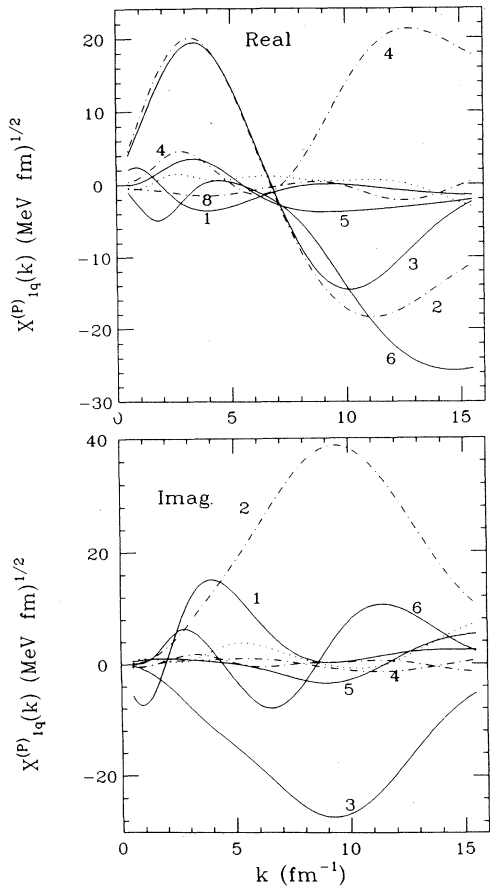

FIG. 6. Form factors of the projection method P, described in Eqs. (D6) and (D7) for the $1\rightarrow 1$ transition for the $^3S_1$-^3D RSC potential, and a center-of-mass energy of 5 MeV. The eigenvalue index q is written next to the curves; the dash-dotted curves represent the results for the positive eigenvalues p_q^P; the dotted lines show the result for the seventh eigenvalue. The eigenvalues are listed in Table VII.

They are normalized by the square root of the eigenvalues $\gamma_t^{(i)}$ in order to satisfy the normalization conditions (D1). The matrix $P^{(n,1)}_{t,t'}$ given by Eq. (D3) is then diagonalized and the resulting eigenvectors and eigenvalues enable one to calculate the form factors F and G in terms of which the representation of O_α is obtained

$$O_\alpha(r,r')=\sum_q F_q^{(\alpha)}(r)G_q^{(\alpha)}(r') \ . \tag{D5}$$

Since the matrix P is not symmetric in the indices t if $n\neq 1$, the right and left eigenvectors of P, R, and L, respectively, will not be the same. In terms of these and of the eigenvalues p_q, the form factors F and G are given by

$$F_q^{(n,1)}(r)=\sum_t V^{(n)}(r)\chi_t^{(n)}(r)R^{(n,1)}_{tq}\sqrt{p_q} \tag{D6}$$

and

$$G_q^{(n,1)}(r)=\sum_t V^{(1)}(r)\chi_t^{(1)}(r)L^{(n,1)}_{qt}\sqrt{p_q} \ . \tag{D7}$$

The eigenvalues p are listed in Table VII, where they are denoted as $p^{(P)}$. Also listed are the quantities $p^{(O)}$. They are defined in a way similar to $p^{(P)}$), with the exception that the projection functions $\chi^{(i)}$ are the Weinberg eigenfunctions for the potential $V_{11}^{(P)}=V_{11}+U_{11}$, and the quantity O_α in Eq. (D3) is equal to $U_{11}+R_{11}^{(P)}$. For comparison, the quantities $\gamma^{(Q)}$ and $\gamma^{(P)}$ are also listed. The former are the eigenvalues of the matrix $V^{(Q)}$ defined by Eq. (3.4) in Q space. They enter in the calculation of the polarization potential U, Eq. (2.11). The quantities $\gamma^{(P)}$ are the Weinberg eigenvalues for the potential $V^{(P)}$, defined in Eq. (2.12), and they enter in the calculation of $R^{(P)}$, Eq. (2.15). The form factors F and G obtained in the projection method by Eqs. (D6) and (D7) are identical to each other in diagonal case where $n=1$. They are illustrated in Fig. 6.

The advantage of the projection procedure P or of the polarization potential method O, as compared to the representation R defined by Eq. (2.7) in the full channel space, is that the size of the matrices which have to be diagonalized are much different. In the P or O methods the size is $M\times M$, while for the full channel space it is $(N\times M)\times(N\times M)$. This advantage should be especially apparent when the number of channels to be eliminated is large. An example could be the calculation of the nucleon-nucleon potential within a channel space which includes various nucleon excited states.[35] The latter then can be represented in terms of a effective potential U which is nonlocal but which is given entirely in the space of the elastic nucleon-nucleon channels.

*On sabbatical leave from the University of Connecticut, Department of Physics, 2152 Hillside Road, Storrs, CT 06268.

[1]W. Plessas, in *Few Body Methods,* edited by T. K. Lim *et al.* (World-Scientific, Singapore, 1986), p. 43; L. S. Ferreira, in *Lecture Notes in Physics,* edited by L. S. Ferreira, A. C. Fonseca, and L. Streit (Springer-Verlag, Berlin, 1987), Vol. 273, p. 100.

[2]S. Weinberg, Phys. Rev. **131**, 440 (1963); M. Scadron and S. Weinberg, *ibid.* **133**, B1589 (1964); R. G. Newton, *Scattering Theory of Waves and Particles* (McGraw-Hill, New York, 1966), pp. 198 and 282.

[3]G. H. Rawitscher, Phys. Rev. C **25**, 2196 (1982).

[4]G. H. Rawitscher (unpublished).

[5]M. K. Srivastava and D. W. Sprung, in *Advances in Nuclear Physics,* edited by M. Baranger and E. Vogt (Plenum, New York, 1975), Vol. 8, p. 121.

[6]J. Haidenbauer, Y. Koike, and W. Plessas, Phys. Rev. C **33**, 439 (1986); Y. Koike, J. Haidenbauer, and W. Plessas, *ibid.* **35**, 396 (1987).

[7]D. Ernst, C. Shakin, and R. Thaler, Phys. Rev. C **8**, 46 (1973); D. Ernst, C. Shakin, R. Thaler, and D. Weiss, *ibid.* **8**, 2056 (1973).

[8]J. Haidenbauer and W. Plessas, Phys. Rev. C **27**, 63 (1983).

[9]B. C. Pearce, Phys. Rev. C **36**, 471 (1987).
[10]E. A. Bartnick, H. Haberzettl, and W. Sandhas, Phys. Rev. C **34**, 1520 (1986); E. A. Bartnick, H. Haberzettl, Th. Januschke, U. Kerwath, and W. Sandhas, *ibid.* **36**, 1678 (1987); T. N. Frank, H. Haberzettl, Th. Januschke, U. Kerwath, and W. Sandhas, *ibid.* **38**, 1122 (1988).
[11]J. S. Ball and D. Y. Wong, Phys. Rev. **169**, 1362 (1968); M. G. Fuda, *ibid.* **186**, 1078 (1969).
[12]T. Brady, M. Fuda, E. Harms, J. S. Levinger, and R. Stagat, Phys. Rev. **186**, 1069 (1969); J. S. Levinger, A. H. Lu, and R. Stagat, *ibid.* **179**, 926 (1969).
[13]G. H. Rawitscher and G. Delic, Phys. Rev. C **29**, 1153 (1984); G. H. Rawitscher, Nucl. Phys. **A475**, 519 (1987).
[14]G. H. Rawitscher and G. Delic, Phys. Rev. **29**, 747 (1984).
[15]G. Delic and G. H. Rawtischer, J. Comput. Phys. **57**, 188 (1985); G. H. Rawitscher and G. Delic, J. Math. Phys. **27**, 186 (1986).
[16]M. Rotenberg, Ann. Phys. (N.Y.) **19**, 262 (1962); M. Fuda, Nucl. Phys. **A116**, 83 (1968); E. Harms, Phys. Rev. C **1**, 1667 (1970); B. Siebert, J. S. Levinger, and E. Harms, Nucl. Phys. **A197**, 33 (1972).
[17]I. R. Afnan and J. M. Read, Phys. Rev. C **8**, 1294 (1973).
[18]A. G. Sitenko and V. F. Kharchenko, Usp. Fiz. Nauk **71**, 469 (1971) [Sov. Phys.—Usp. **14**, 125 (1971)]; A. G. Sitenko, V. F. Kharchenko, and N. M. Petrov, Phys. Lett. **28B**, 308 (1968).
[19]G. Pisent and L. Canton, Nuovo Cimento **91A**, 33 (1986); L. Canton, G. Cattapan, and G. Pisent, *ibid.* **97A**, 319 (1987).
[20]L. Canton, G. Cattapan, and G. Pisent, Nucl. Phys. **A487**, 333 (1988).
[21]S. Sofiancos, H. Fiedeldey, and N. J. McGurk, Nucl. Phys. **A294**, 49 (1978).
[22]R. C. Fuller, Phys. Rev. **118**, 1649 (1969); M. Baldo, L. Ferreira, and L. Streit, *ibid.* **118**, 1649 (1969); Phys. Rev. C **36**, 1743 (1987); Nucl. Phys. **A467**, 44 (1987).
[23]B. Gyarmati, A. Kruppa, and J. Revai, Nucl. Phys. **A326**, 119 (1979); B. Gyarmati and A. Kruppa, Phys. Rev. C **34**, 95 (1986).
[24]K. Hartt and P. V. A. Yidana, Phys. Rev. C **36**, 475 (1987).
[25]S. K. Adhikari and L. Tomio, Phys. Rev. C **36**, 1275 (1987).
[26]S. Adhikari and I. Sloan, Phys. Rev. C **11**, 1133 (1975); Nucl. Phys. **A241**, 429 (1975).
[27]M. I. Haftel and F. Tabakin, Nucl. Phys. **A158**, 1 (1970).
[28]L. Canton, G. Pisent, and G. Rawitscher (unpublished).
[29]E. O. Alt and W. Sandhas, Phys. Rev. C **18**, 1088 (1979).
[30]L. Canton and G. Pisent, Acta Pys. Austriaca, Suppl. **XXVII**, 645 (1985); in *Proceedings of the Primo covengo su problemi di fisica nucleare teorica,* edited by L. Bracci *et al.* (Cortona, Italy, 1985), p. 75.
[31]R. A. Brandenburg, G. S. Chulik, R. Machleidt, A. Picklesimer, and R. M. Thaler, Phys. Rev. C **38**, 1397 (1988).
[32]R. V. Reid, Ann. Phys. (N.Y.) **50**, 411 (1968).
[33]M. Abramowitz and I. Stegun, *Handbook of Mathematical Functions* (Dover, New York, 1972), Sec. 5.
[34]E. F. Redish and K. Stricker-Bauer, Phys. Rev. C **36**, 513 (1987).
[35]A. M. Green and M. E. Saino, J. Phys. G **5**, 503 (1979); E. L. Lomon, Phys. Rev. D **26**, 576 (1982); T. S. H. Lee, Phys. Rev. C **29**, 195 (1983); T. S. H. Lee and A. Matsuyama, *ibid.* **36**, 1459 (1987); R. Machleidt, K. Holinde, and Ch. Elster, Phys. Rep. **149**, 1 (1978); H. Döpping and P. U. Sauer, in *Progress in Particle and Nuclear Physics,* edited by A. Faessler (Plenum, New York, 1986), Vol. 16, p. 355; G. Q. Liu and F. Tabakin, Bull. Am. Phys. Soc. **33**, 1023 (1988).